INTERNATIONAL JOURNAL FOR NUMERICAL METHODS IN ENGINEERING
Int. J. Numer. Meth. Engng 2002; **53**:751–763 (DOI: 10.1002/nme.313)

A hybrid boundary node method

Jianming Zhang[1,*,†], Zhenhan Yao[1] and Hong Li[2]

[1] *Department of Engineering Mechanics, Tsinghua University, Beijing 100084, People's Republic of China*
[2] *Shashi Steel Pipe Works, Jingzhou, Hubei 434001, People's Republic of China*

SUMMARY

A new variational formulation for boundary node method (BNM) using a hybrid displacement functional is presented here. The formulation is expressed in terms of domain and boundary variables, and the domain variables are interpolated by classical fundamental solution; while the boundary variables are interpolated by moving least squares (MLS). The main idea is to retain the dimensionality advantages of the BNM, and get a truly meshless method, which does not require a 'boundary element mesh', either for the purpose of interpolation of the solution variables, or for the integration of the 'energy'. All integrals can be easily evaluated over regular shaped domains (in general, semi-sphere in the 3-D problem) and their boundaries.

Numerical examples presented in this paper for the solution of Laplace's equation in 2-D show that high rates of convergence with mesh refinement are achievable, and the computational results for unknown variable are most accurate. No further integrations are required to compute the unknown variables inside the domain as in the conventional BEM and BNM. Copyright © 2001 John Wiley & Sons, Ltd.

KEY WORDS: meshless methods; hybrid boundary node method; moving least-squares approximation

1. INTRODUCTION

Although the FEM and BEM have made great achievements in solving practical engineering problems, the interest of pursuing new methods has never decreased through time, as the mesh-based methods (e.g. FEM and BEM) have much difficulty in solving problems involving changing domains such as large deformation or crack propagation; and the task of mesh generation of a 3-D object with complicated geometry is often arduous, time-consuming and computationally expensive, in spite of this significant progress has been made in 3-D meshing algorithms. In recent years, novel computational algorithms, referred to as 'meshless' methods, have been proposed, that largely circumvent the problems associated with meshing.

The initial idea of meshless methods dates back to the smooth particle hydrodynamics (SPH) method for modelling astrophysical phenomena [1] while the research into meshless methods

*Correspondence to: Jianming Zhang, Room 402, Building 20, Tsinghua University, Beijing 100084, People's Republic of China
†E-mail: zhangjm00@mails.tsinghua.edu.cn

Received 18 July 2000
Revised 9 February 2001

became active only after the publishing of the diffuse element method by Nayroles *et al.* [2] and the element-free Galerkin method by Belytschko *et al.* [3]. The element-free Galerkin (EFG) method uses a global symmetric weak form and the shape functions from the moving least-squares approximation. Although no mesh is required in the EFG method for the interpolation of the solution variables, background cells are inevitable for the integration of 'energy'.

Recently, two meshless methods, the meshless local boundary integral equation (MLBIE) method by Zhu *et al.* [4, 5] and the meshless local Petrov–Galerkin (MLPG) approach by Atluri *et al.* [6] have been developed. Both methods use local weak forms over a local subdomain and shape functions from the MLS approximation, and lead to truly meshless ones, as no 'finite element or boundary element mesh' is required either for the purpose of interpolation of the solution variables, or for the integration of the 'energy'. All integrals can be easily evaluated over regularly shaped domains (for example, circles in 2-D problems and spheres in 3-D problems) and their boundaries.

Most recently, Mukherjee and Mukherjee [7] proposed a meshless method, which they call the boundary node method (BNM). They combined the MLS interpolants with boundary integral equations (BIE) in order to retain both the meshless attribute of the former and the dimensionality advantage of the latter. This method only requires a nodal data structure on the bounding surface of a body whose dimension is one less than that of the domain itself; but this method is not a truly meshless one, as an underlying cell structure is again used for numerical integration.

A question arises here—is there possibly a method of solving boundary value problems, that only requires nodes distributed on the surface of a domain and require no cells either for the interpolation of the solution variables or for the numerical integration? This method will simplify the input data structure greatly, as it has the dimensionality advantage of the BIE and only requires scattered nodes on boundary of the domain, compared with the MLBIE and MLPG; and it is a truly meshless method, which does not use any mesh either for interpolation or for integration, compared with the BNM.

The answer is positive. The new method is called Hybrid boundary node method (Hybrid BNM), which combines the MLS interpolation scheme with the hybrid displacement variational formulation, and this is the subject of the present paper.

The hybrid boundary element method was first proposed by Schnack [8], in which he stressed using the boundary element method to generate a hybrid stress finite element model, giving rapid convergence of the results and accurate solution for stress concentration problems. Dumont [9] has presented a hybrid stress boundary element formulation based on Hellinger–Reissner's principle with stresses in the domain and displacements on the boundary as independent functions. DeFigueredo and Brebbia [10] have introduced a hybrid displacement variational formulation of BEM, which is based on a modified functional using three independent variables, i.e. displacements and tractions on the boundary and displacements inside the domain. This approach uses the classical fundamental solution to interpolate the displacements in the domain and thus allowing for the transfer of the domain integrals to the boundary. The resulting system of equations is written in terms of boundary displacements only, and has the advantage of being symmetrical, which is easy to couple with the FEM. In the present paper, the objective is not to obtain the symmetrical system of equations in terms of boundary displacements, we just use the hybrid displacement variational formulation and the interpolation scheme of variables inside the domain. The variables on the boundary are interpolated by MLS scheme and a truly meshless Hybrid BNM is achieved.

The following discussion begins with the brief description of the MLS approximation in Section 2. Taking Laplace equation as an example, the Hybrid BNM and its meshless implementation are presented in Section 3. Numerical examples for 2-D potential problems are given in Section 4. The paper ends with conclusions and discussions in Section 5.

2. THE MLS APPROXIMATION SCHEME FOR THE 2-D HBNM

This section gives a brief summary of the MLS approximation, of which excellent illustrations can be seen in References [11, 12].

The discussion below addresses the solution u of a scalar problem (Laplace's equation) in 2-D. In the view of the fact that this MLS interpolation scheme will be coupled later with 2-D hybrid 'displacement' variational formulation which uses three independent variables, of which the $\tilde{u}$ and $\tilde{q}$ are defined as the potential and normal flux on the 1-D bounding surface Γ of a 2-D body Ω, and will be interpolated by MLS scheme.

The difference in MLS interpolation between the present approach and the BNM [7] is that in the present approach, MLS interpolation is independently performed on piecewise smooth segments $\Gamma_i,\ i=1,2,\ldots,n$ which consist of the boundary naturally other than the whole boundary Γ. To approximate the functions $\tilde{u}$ and $\tilde{q}$ on each Γ_i, over which a number of randomly located nodes $\{s_I\},\ I=1,2,\ldots,N$, the MLS interpolants for $\tilde{u}$ and $\tilde{q}$ are defined as

$$\tilde{u}(s)=\sum_{j=1}^{m} p_j(s)a_j(s)=\mathbf{p}^{\mathrm{T}}(s)\mathbf{a}(s) \tag{1}$$

$$\tilde{q}(s)=\sum_{j=1}^{m} p_j(s)b_j(s)=\mathbf{p}^{\mathrm{T}}(s)\mathbf{b}(s) \tag{2}$$

where s is a curvilinear co-ordinate (here the arc length) on $\Gamma_i,\ p_1=1$ and $p_j(s),\ j=2,\ldots,m$ are monomials in s. The monomials $p_j(s)$ provide the intrinsic polynomial bases for $\tilde{u}$ and $\tilde{q}$. In the numerical implementation presented later in this paper, a quadratic background basis is used, i.e.

$$\mathbf{p}^{\mathrm{T}}(s)=[1,s,s^2],\quad m=3 \tag{3}$$

The coefficient vector $\mathbf{a}(s)$ and $\mathbf{b}(s)$ is determined by minimizing a weighted discrete L_2 norm, defined as

$$J_1(s)=\sum_{I=1}^{N} w_I(s)[\mathbf{p}^{\mathrm{T}}(s_I)\mathbf{a}(s)-\hat{u}_I]^2 \tag{4}$$

$$J_2(s)=\sum_{I=1}^{N} w_I(s)[\mathbf{p}^{\mathrm{T}}(s_I)\mathbf{b}(s)-\hat{q}_I]^2 \tag{5}$$

where points s_I are boundary nodes on $\Gamma_i,\ s$ is the co-ordinate of an evaluation point E, which can either be a source point P (a boundary node on Γ_i) or a field point Q (a Gauss point on Γ_i) in the present approach, N is the number of boundary nodes in the neighbourhood of E for which the weight functions $w(s-s_I)>0$. It should be noted here that $\hat{u}_I$ and $\hat{q}_I,\ I=1,2,\ldots,N$ are the fictitious nodal values other than the nodal values of the unknown $\tilde{u}_I$ and $\tilde{q}_I$ in general.

This distinction between $\hat{u}_I$ and $\tilde{u}_I$ (or $\hat{q}_I$ and $\tilde{q}_I$) is very important in the view of the fact that MLS interpolants lack the delta function property.

Solving for $\mathbf{a}(s)$ and $\mathbf{b}(s)$ by minimizing J_1 and J_2 in Equations (4) and (5), and substituting them into Equations (1) and (2) gives a relation which may be written in the form of an interpolation function similar to that used in the FEM, as

$$\tilde{u}(s) = \sum_{I=1}^{N} \Phi_I(s)\hat{u}_I \tag{6}$$

$$\tilde{q}(s) = \sum_{I=1}^{N} \Phi_I(s)\hat{q}_I \tag{7}$$

where

$$\Phi_I(s) = \sum_{j=1}^{m} p_j(s)A^{-1}(s)B(s)]_{jI} \tag{8}$$

with the matrices $A(s)$ and $B(s)$ being defined by

$$A(s) = \sum_{I=1}^{N} w_I(s)\mathbf{p}(s_I)\mathbf{p}^{\mathrm{T}}(s_I) \tag{9}$$

$$B(s) = [w_1(s)\mathbf{p}(s_1), w_2(s)\mathbf{p}(s_2), \ldots, w_N(s)\mathbf{p}(s_N)] \tag{10}$$

The MLS approximation is well defined only when the matrix A in Equation (9) is non-singular.

$\Phi_I(s)$ is usually called the shape function of the MLS approximation corresponding to nodal point s_I. From Equations (8) and (10), it may be seen that $\Phi_I(s) = 0$ when $w_I(s) = 0$. The fact that $\Phi_I(s)$ vanishes for s not in the support of nodal point s_I preserves the local character of the MLS approximation.

Several kinds of weight function can be seen in the literatures, the choice of weight functions and the consequences of a choice in the EFG method are discussed in some detail elsewhere [11]. Gaussian weight function corresponding to node s_I may be written as

$$w_I(s) = \begin{cases} \dfrac{\exp[-(d_I/c_I)^2] - \exp[-(\hat{d}_I/c_I)^2]}{1 - \exp[-(\hat{d}_I/c_I)^2]}, & 0 \leqslant d_I \leqslant \hat{d}_I \\ 0, & d_I \geqslant \hat{d}_I \end{cases} \tag{11}$$

where $d_I = |s - s_I|$ is the absolute value of the distance between an evaluation point and a node, measured along Γ_i, c_I is a constant controlling the shape of the weight function, and $\hat{d}_I$ is the size of the support for the weight function w_I and determines the support of node s_I. The $\hat{d}_I$ should be chosen such that $\hat{d}_I$ should be large enough to have sufficient number of nodes covered in the domain of definition of every sample point ($N \geqslant m$) to ensure the regularity of A.

3. DEVELOPMENT OF THE HYBRID BOUNDARY NODE METHOD

In this section, the development of the Hybrid BNM is illustrated by the following potential problem:

$$\begin{aligned} u_{,ii} &= 0 \quad \forall x \in \Omega \\ u &= \bar{u} \quad \forall x \in \Gamma_u \\ u_{,i}\, n_i \equiv q &= \bar{q} \quad \forall x \in \Gamma_q \end{aligned} \tag{12}$$

where the domain Ω is enclosed by $\Gamma = \Gamma_u + \Gamma_q$, $\bar{u}$ and $\bar{q}$ are the prescribed potential and normal flux, respectively, on the essential boundary Γ_u and on the flux boundary Γ_q, and n is the outward normal direction to the boundary Γ, with n_i components.

The Hybrid BNM proposed in this paper is based on a modified variational principle. The functions assumed to be independent are:

— potential field in the domain, u;
— boundary potential field, $\tilde{u}$;
— boundary normal flux, $\tilde{q}$.

The corresponding variational functional Π_{AB} is defined as follows:

$$\Pi_{AB} = \int_\Omega \tfrac{1}{2}\, u_{,i}\, u_{,i}\, \mathrm{d}\Omega - \int_\Gamma \tilde{q}(u - \tilde{u})\, \mathrm{d}\Gamma - \int_{\Gamma_q} \bar{q}\tilde{u}\, \mathrm{d}\Gamma \tag{13}$$

where the boundary potential $\tilde{u}$ satisfies the essential boundary condition, i.e., $\tilde{u} = \bar{u}$ on Γ_u.

By carrying out the variations it can be shown that

$$\delta\Pi_{AB} = \int_\Gamma (q - \tilde{q})\delta u\, \mathrm{d}\Gamma - \int_\Omega u_{,ii}\, \delta u\, \mathrm{d}\Omega + \int_{\Gamma_q} (\tilde{q} - \bar{q})\delta\tilde{u}\, \mathrm{d}\Gamma - \int_\Gamma (u - \tilde{u})\delta\tilde{q}\, \mathrm{d}\Gamma \tag{14}$$

The vanishing of $\delta\Pi_{AB}$ for arbitrary variations δu in Ω, $\delta\tilde{u}$ and $\delta\tilde{q}$ on Γ, with $\delta\tilde{u} = 0$ on Γ_u, gives the following Euler equations:

$$\begin{aligned} u_{,ii} &= 0, \quad \text{in } \Omega \\ u - \tilde{u} &= 0, \quad \text{on } \Gamma \\ q - \tilde{q} &= 0, \quad \text{on } \Gamma \\ \tilde{q} - \bar{q} &= 0, \quad \text{on } \Gamma_q \end{aligned} \tag{15}$$

Consequently, the solution of the problem is now given in terms of the functions u, $\tilde{u}$ and $\tilde{q}$, which make $\delta\Pi_{AB}$ stationary.

With the vanishing of $\delta\Pi_{AB}$, one can also have the following equivalent integral equations:

$$\int_\Gamma (q - \tilde{q})\delta u\, \mathrm{d}\Gamma - \int_\Omega u_{,ii}\, \delta u\, \mathrm{d}\Omega = 0 \tag{16}$$

$$\int_\Gamma (u - \tilde{u})\delta\tilde{q}\, \mathrm{d}\Gamma = 0 \tag{17}$$

$$\int_{\Gamma_q} (\tilde{q} - \bar{q})\delta\tilde{u}\, \mathrm{d}\Gamma = 0 \tag{18}$$

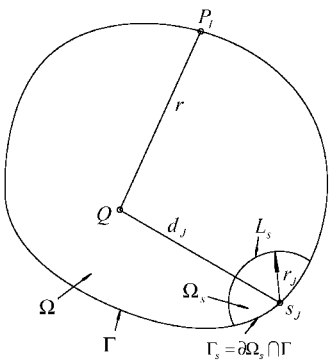

Figure 1. The domain Ω and the sub-domain Ω_s of nodes s_J.

If we impose the flux boundary condition, $\tilde{q} = \bar{q}$, just the same way as the essential boundary condition after the matrices have been computed, Equation (18) will be satisfied. So it can be ignored temporarily in the following development.

It can be seen that Equations (16) and (17) hold in any sub-domain, for example, in a sub-domain Ω_s and its boundary Γ_s and L_s (see Figure 1). The following developing idea is from References [5, 6]. In fact, to follow the developing process in References [5, 6], we use the following weak forms on a sub-domain Ω_s and its boundary Γ_s and L_s to replace Equations (16) and (17):

$$\int_{\Gamma_s + L_s} (q - \tilde{q}) v \, d\Gamma - \int_{\Omega_s} u_{,ii} \, v \, d\Omega = 0 \tag{19}$$

$$\int_{\Gamma_s + L_s} (u - \tilde{u}) v \, d\Gamma = 0 \tag{20}$$

where v is a test function. It should be noted further that the above equations hold irrespective of the size and the shape of Ω_s and its boundary $\partial\Omega_s$. This is an important observation, which forms the basis for the following development. We now deliberately choose a simple regular shape for Ω_s. The most regular shape of a sub-domain should be an n-dimensional sphere for a boundary value problem defined on an n-dimensional space. In the present paper, the sub-domain Ω_s is chosen as the intersection of the domain Ω and a circle centred at a boundary node s_J (see Figure 1).

In Equations (19) and (20), $\tilde{u}$ and $\tilde{q}$ on Γ_s are expressed by Equations (6) and (7), but $\tilde{u}$ and $\tilde{q}$ on L_s has not been defined yet. To solve this problem, we deliberately select v such that all integrals vanish on L_s. This can be easily accomplished by using the weight function in the MLS approximation as v, with the radius $\hat{d}_I$ of the support of the weight function being replaced by the radius r_J of the sub-domain Ω_s as that in Reference [5], for example, for a node s_J:

$$v_J(Q) = \begin{cases} \dfrac{\exp[-(d_J/c_J)^2] - \exp[-(r_J/c_J)^2]}{1 - \exp[-(r_J/c_J)^2]}, & 0 \leqslant d_J \leqslant r_J \\ 0, & d_J \geqslant r_J \end{cases} \tag{21}$$

where d_J is the distance between a point Q, in domain Ω, and the nodal point s_J. Therefore, $v_J(Q)$ vanishes on L_s.

The u and q inside Ω and on Γ are defined as

$$u = \sum_{I=1}^{n} U_I x_I \tag{22}$$

$$q = \sum_{I=1}^{n} \frac{\partial U_I}{\partial n} x_I \tag{23}$$

where U_I is the fundamental solution with source point at a node P_I, $U_I = (-1/2\pi)\ln r(Q, P_I)$; x_I are unknown parameters; n is the total number of boundary nodes.

As u is expressed by Equation (22), the last integral on the left-hand side of Equation (19) vanishes if one excludes node s_J from the sub-domain Ω_s at which the singularity occurs. This singularity will be considered when evaluating the boundary integrals.

By substituting Equations (6), (7), (21), (22) and (23) into Equations (19) and (20), and omitting the vanished terms, one has

$$\begin{aligned} \sum_{I=1}^{n} \int_{\Gamma_s} \frac{\partial U_I}{\partial n} v_J(Q) x_I \, \mathrm{d}\Gamma &= \sum_{I=1}^{n} \int_{\Gamma_s} \Phi_I(s) v_J(Q) \hat{q}_I \, \mathrm{d}\Gamma \\ \sum_{I=1}^{n} \int_{\Gamma_s} U_I v_J(Q) x_I \, \mathrm{d}\Gamma &= \sum_{I=1}^{n} \int_{\Gamma_s} \Phi_I(s) v_J(Q) \hat{u}_I \, \mathrm{d}\Gamma \end{aligned} \tag{24}$$

In the present formulation, it is much important to choose the integration regions Γ_s properly. This is really true for 3-D problems [13, 14]. Theoretically, the ideal condition is that they cover the boundary of the body and do not overlap. However, from our computation, the present formulation can give acceptable results even when the union of all local regions Γ_s does not cover the whole boundary, although the best condition is that every region Γ_s is as large as possible, as long as the region Γ_s includes only one node. This brings much convenience in choosing integration regions, Γ_s, in the 3-D situation.

Using Equations (24) for all nodes, we obtain the final system of equations:

$$\mathbf{U}\mathbf{x} = \mathbf{H}\hat{\mathbf{q}} \tag{25}$$

$$\mathbf{V}\mathbf{x} = \mathbf{H}\hat{\mathbf{u}} \tag{26}$$

where

$$U_{IJ} = \int_{\Gamma_s^J} \frac{\partial U_I}{\partial n} v_J(Q) \, \mathrm{d}\Gamma$$

$$V_{IJ} = \int_{\Gamma_s^J} U_I v_J(Q) \, \mathrm{d}\Gamma$$

$$H_{IJ} = \int_{\Gamma_s^J} \Phi_I(s) v_J(Q) \, \mathrm{d}\Gamma$$

$$\mathbf{x}^{\mathrm{T}} = [x_1, x_2, \ldots, x_n]$$

$$\hat{\mathbf{q}}^{\mathrm{T}} = [\hat{q}_1, \hat{q}_2, \ldots, \hat{q}_n]$$

$$\hat{\mathbf{u}}^{\mathrm{T}} = [\hat{u}_1, \hat{u}_2, \ldots, \hat{u}_n]$$

From Equation (25) we have

$$\mathbf{x} = \mathbf{V}^{-1}\mathbf{H}\hat{\mathbf{u}} \tag{27}$$

Substitute Equation (27) into Equation (26), we have

$$\mathbf{U}\mathbf{V}^{-1}\mathbf{H}\hat{\mathbf{u}} - \mathbf{H}\hat{\mathbf{q}} = 0 \tag{28}$$

The evaluation of the matrix $\mathbf{U}$ is the more critical step in this approach, as integrations of singular functions are required. Accurate and appropriate numerical integration schemes have to be used for different types of singularities that occur. However, the main diagonal of matrix $\mathbf{U}$ can be calculated by applying a special solution (e.g. constant field), therefore, avoiding the evaluation of hyper singular integrals.

The equations can be solved in the same way as in the conventional BEM, except that transformations between $\hat{u}_I$ and $\tilde{u}_I$, $\hat{q}_I$ and $\tilde{q}_I$ must be performed, due to that the MLS interpolants lack the delta function property of the usual BEM shape functions (see Reference [15]).

On the edges on which u are prescribed, $\hat{u}_I$ can be obtained by following transformation:

$$\hat{u}_I = \sum_{J=1}^{N} R_{IJ}\tilde{u}_J = \sum_{J=1}^{N} R_{IJ}\bar{u}_J \tag{29}$$

On the edges on which q are prescribed, $\hat{q}_I$ can be obtained by the same transformation as (29):

$$\hat{q}_I = \sum_{J=1}^{N} R_{IJ}\tilde{q}_J = \sum_{J=1}^{N} R_{IJ}\bar{q}_J \tag{30}$$

where $R_{IJ} = [\Phi_J(s_I)]^{-1}$.

The unknown vector $\mathbf{x}$ can be obtained by Equation (27) after Equation (28) has been solved. Potential u and flux q at any point inside domain Ω can be evaluated by Equations (22) and (23) without further integrations. Potential $\tilde{u}$ and flux $\tilde{q}$ on boundary Γ can be evaluated by Equations (6) and (7).

From the above development, one can see that the present method is a truly meshless one, as absolutely no boundary elements are needed, either for interpolation purpose or for integration purpose. Although one more matrix and one more equation need to be calculated and solved compared with BNM, the matrix $\mathbf{H}$ is very easily obtained since it is a very sparse matrix, and no further integration is needed in the 'post-processing' step.

4. ILLUSTRATIVE NUMERICAL RESULTS

A few illustrative numerical results from the Hybrid BNM, together with comparisons with exact solutions, follow. In all cases, the Laplace equation

$$\nabla^2 u = 0$$

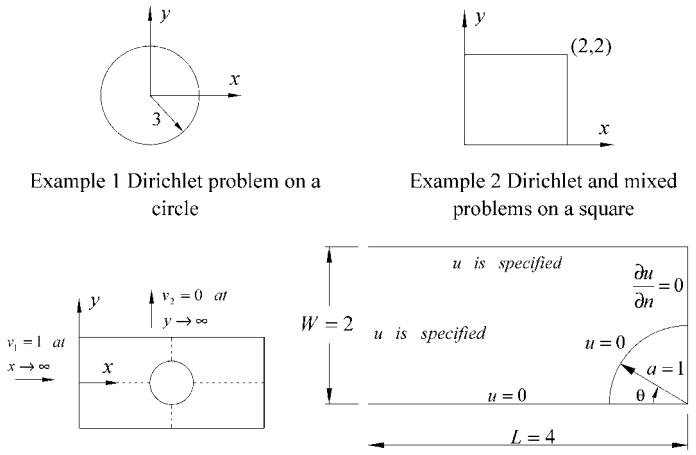

Figure 2. Geometry and boundary conditions for the examples.

is solved, together with appropriate prescribed boundary conditions. For the purpose of error estimation and convergence studies, a 'global' L_2 norm error, normalized by $|u|_{\max}$ is defined as

$$e = \frac{1}{|u|_{\max}} \sqrt{\frac{1}{N} \sum_{i=1}^{N} \left(\mathbf{u}_i^{(\mathrm{e})} - \mathbf{u}_i^{(\mathrm{n})}\right)^2} \tag{31}$$

where $|u|_{\max}$ is the maximum value of u over N sample points, the superscripts (e) and (n) refer to the exact and numerical solutions, respectively.

In the first two examples, the size of support for weight function, $\hat{d}_I$ in Equation (11), is taken to be $3.5h$, with h being the mesh size, and the parameter c_I in Equation (11) is taken to be such that $\hat{d}_I/c_I$ is constant and equal to 1.0. The size (radius r_J) of the local domain for each node is chosen as $0.9h$ and the parameter c_J in Equation (21) is taken to be such that r_J/c_J is constant and equal to 1.2. Also, in all integrations, 5 Gauss points are used on each part of two sections of Γ_s.

Example 1 (*Dirichlet problem on a circle*). The example solved here is the Laplace equation on a circle of radius 3 unit, centred at the origin (see Figure 2). The exact solution is

$$u = x \tag{32}$$

A Dirichlet problem is solved, for which the essential boundary condition is imposed on the whole circle. To study the convergence of the present method, three regular meshes of 100, 140 and 180 nodes have been used (see Figure 2). Numerical results of u and q (with normal vector (1,0)) along the radius (from (0,0) to (3,0)) from the Hybrid BNM, together with the exact solution, are shown in Figure 3.

Results for potentials are in all case accurate. The internal fluxes, however, show considerable error for points close to the boundary when a small number of nodes are used. The same 'boundary layer effect' has been observed in other hybrid BEM calculations as well [10].

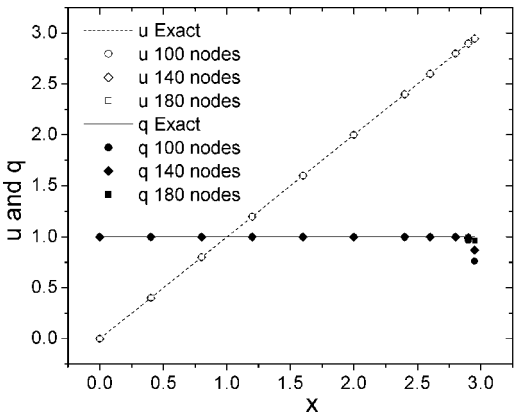

Figure 3. u and q along the radius (from (0,0) to (3,0)).

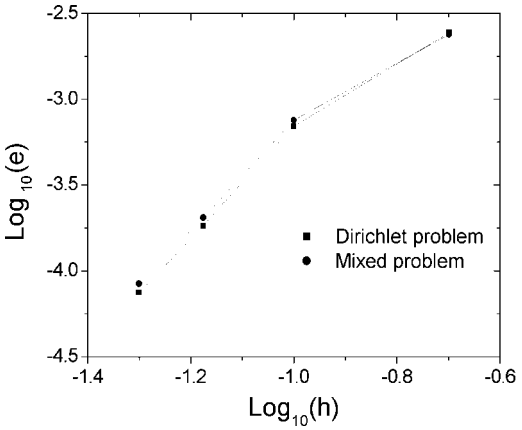

Figure 4. Relative errors and convergence rates for the Dirichlet and mixed problems on a square.

This is to be expected as they are calculated as a superposition of fundamental solutions of higher order of singularity than the ones used for the potentials (Equations (22) and (23)). The results improved considerably when the number of nodes increased in the vicinity of the internal point. It is recommended that the ratio between h, closest to the internal point, and the distance from that point to the boundary be no greater than 0.5. Anyhow, this is a main pitfall of the present method and other hybrid BEM models. Further study on this point is underway.

Example 2 (*Dirichlet and mixed problem on a square*). The case of Laplace equation on a 2×2 domain is presented as the second example, see Figure 2. The exact solution is a cubic polynomial

$$u = -x^3 - y^3 + 3x^2y + 3xy^2 \tag{33}$$

A Dirichlet problem is solved for which the essential boundary condition is imposed on all edges, and a mixed problem for which the essential boundary condition is imposed on top and bottom edges and the flux boundary condition is prescribed on left and right edges of the domain.

To study the convergence of the method, four different regular nodes arrangements of 10, 20, 30 and 40 nodes on each edge have been used. The results of relative errors (Equation (31)) and convergence of potential on the diagonal (from (0,0) to (2,2), 19 uniformly spaced sample points) are shown in Figure 4, and numerical results of normal flux on the edge (from (0,0) to (2,0)) from the Hybrid BNM, together with the exact solution are shown in Figure 5.

It can be seen that the present Hybrid BNM has high rates of convergence and the agreement between numerical and exact results are excellent.

Example 3 (*Potential flow*). The third example considered here is the problem of a potential flow around a cylinder of radius 1 in an infinite domain, u represents the stream function.

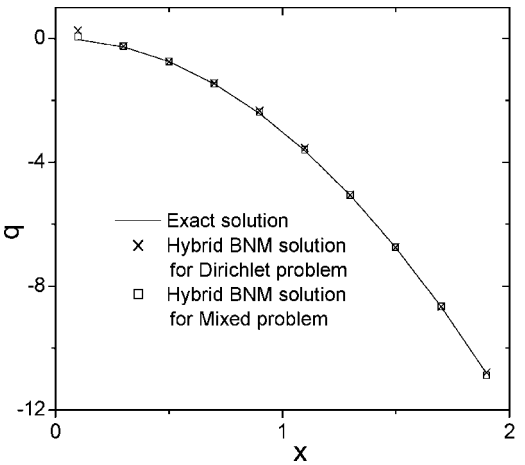

Figure 5. $q(x)$ on $y=0$ for the Dirichlet and mixed problems on a square (20 nodes on each side).

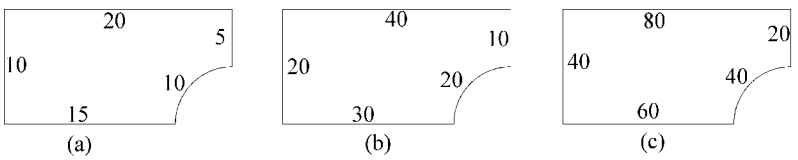

Figure 6. Flow around a cylinder: nodal arrangement: (a) 60 nodes; (b) 120 nodes; (c) 240 nodes.

Due to the symmetry of the problem, only a part, $0 \leqslant x \leqslant 4$ and $0 \leqslant y \leqslant 2$, of the upper left quadrant of the field is modelled as shown in Figure 2. The exact solution for this problem is given by

$$u = y\left[1 - \frac{a^2}{y^2 + (x-L)^2}\right] \tag{34}$$

The prescribed u and q values along all boundaries are shown in Figure 2. The essential boundary condition on the left and top edges is imposed according to the exact solution. The nodes arranged on each edge are shown in Figure 6. In the nodes arrangements (a), (b) and (c), the size of support for weight function, $\tilde{d}_I$ in Equation (11), is taken to be $3h$, $5h$ and $10h$, with h being the mesh size, respectively. Other parameters are the same as those used in the first two examples.

To study how the local sub-domain size (radius r_J) affects the solution accuracy of the present method, three different cases with $r_J = 0.3h$, $0.5h$ and $0.9h$ for each node, have been considered. Numerical results, when $r_J = 0.9h$, from the Hybrid BNM along the arc (from (3,0) to (4,1)), together with the exact solution, are shown in Figure 7. The results of relative errors (Equation (31)) and convergence of potential on the diagonal (from (0,0) to (4,2),

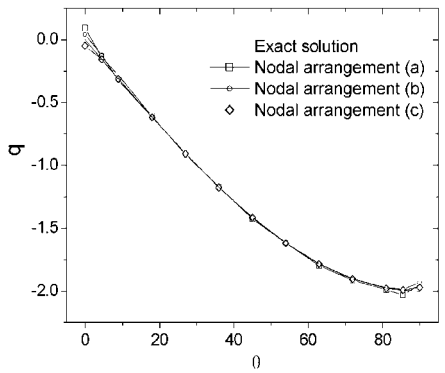

Figure 7. $q(\theta)$ on the arc with different nodes arrangements.

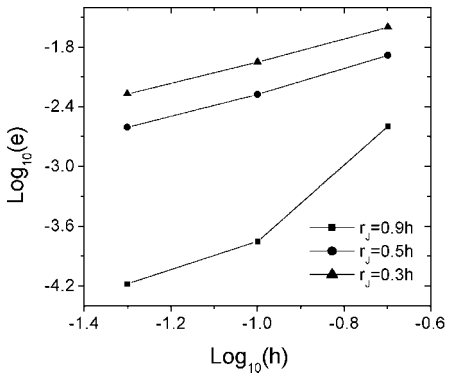

Figure 8. Relative errors and convergence rates for the potential flow problem.

19 uniformly spaced sample points) are shown in Figure 8. The numerical results agree excellently with the exact solutions again, and high rates of convergence are achieved. From Figure 8, the best size for each node is $r_J = 0.9h$ (sub-domains overlapped each other), while the Hybrid BNM still yields acceptable results when $r_J = 0.3h$ and $0.5h$.

5. CONCLUSIONS AND DISCUSSIONS

A new type of boundary nodes method has been presented in this paper. It is based on a hybrid model that involves three types of independent variables, i.e. potentials and normal fluxes on the boundary and potentials inside the domain, and coupled with the MLS interpolation scheme over the boundary variables. Compared with the MLBIE and MLPG, the new approach has the well-known dimensionality of the BEM, i.e. for a 3-D object, only randomly distributed nodal points are required to be constructed on the 2-D bounding surface of a body; compared with the conventional BEM, it is a meshless method, only requires a nodal data structure on the bounding surface of the domain to be solved; compared with the BNM, it is a truly meshless method, absolutely no cells are needed either for interpolation purpose or for integration purpose.

Numerical examples have shown the accuracy and convergence of the results. The solution is most accurate for the potentials and fluxes on the boundary and in the domain. High rates of convergence have been achieved. The calculation of variables at internal points does not demand the evaluation of any integrals as in the conventional BEM or the BNM.

The most exciting feature of the Hybrid BNM, perhaps, is that it can directly use a solid model for 3-D object without any meshing. Therefore, it can be interlinked with CAD software very easily and offers very promising applications in practical engineering. The only drawback of the Hybrid BNM is its serious 'boundary layer effect'. How to avoid this pitfall is a planned investigation for the future. Nevertheless, the advantages are so attractive that this method deserves consideration.

REFERENCES

1. Lucy LB. A numerical approach to the testing of the fission hypothesis. *The Astronomy Journal* 1977; **8**: 1013–1024.
2. Nayroles B, Touzot G, Villon P. Generalizing the finite element method: diffuse approximation and diffuse element. *Computational Mechanics* 1992; **10**:307–318.
3. Belytschko T, Lu YY, Gu L. Element free Galerkin methods. *International Journal for Numerical Methods in Engineering* 1994; **37**:229–256.
4. Zhu T, Zhang J, Atluri SN. A local boundary integral equation (LBIE) method in computation mechanics, and a meshless discretization approach. *Computational Mechanics* 1998; **21**:223–235.
5. Zhu T. A new meshless regular local boundary integral equation (MRLBIE) approach. *International Journal for Numerical Methods in Engineering* 1999; **46**:1237–1252.
6. Atluri SN, Zhu T. A new meshless local Petrov–Galerkin approach in computational mechanics. *Computational Mechanics* 1998; **22**:117–127.
7. Mukherjee YX, Mukherjee S. The boundary node method for potential problems. *International Journal for Numerical Methods in Engineering* 1997; **40**:797–815.
8. Schnack E. A hybrid BEM model. *International Journal for Numerical Methods in Engineering* 1987; **24**: 1015–1025.
9. Dumount NA. The hybrid boundary element method. *Proceedings of the Nineth International Conference on BEM*, Stuttgart. Computational Mechanics Publications: Southampton and Springer-Verlag, Berlin, 1987.
10. DeFigueredo TGB, Brebbia CA. A new hybrid displacement variational formulation of BEM for elastostatics. Advances in Boundary Elements, In Brebbia CA, Conner JJ (eds). Computational Mechanics Publications, Southampton, 1989; Vol **1**:47–57.
11. Belytschko T, Krongauz Y, Organ D, Fleming M, Krysl P. Meshless methods: an overview and recent developments. *Computer Methods in Applied Mechanics and Engineering* 1996; **139**:3–47.
12. Lancaster P, Salkauskas K. Surfaces generated by moving least squares methods. *Mathematics in Computation* 1981; **37**:141–158.
13. Chati MK, Mukherjee S, Mukherjee YX. The boundary node method for three-dimensional linear elasticity. *International Journal for Numerical Methods in Engineering* 1999; **46**:1163–1184.
14. Chati MK, Mukherjee S. The boundary node method for three-dimensional problems in potential theory. *International Journal for Numerical Methods in Engineering* 2000; **47**:1523–1547.
15. Atluri SN, Kim HG, Cho JY. A critical assessment of the truly meshless local Petrov–Galerkin (MLPG), and local boundary integral equation (LBIE) methods. *Computational Mechanics* 1999; **24**:348–372.

